

# GREEN SYNTHESIS AND CHARACTERIZATION OF NANOCOMPOSITES

N. Tensingh Baliah<sup>1</sup>, P. Muthulakshmi<sup>2</sup>, P. Celestin Sheeba<sup>3</sup>, S. Lega Priyatharsini<sup>4</sup>

<sup>1,2,3,4</sup>Center for Research and Post Graduate studies in Botany, Ayya Nadar Janaki Ammal College, Sivakasi, Tamil Nadu, India.

\*\*\*

**ABSTRACT:-** The present investigation has been aimed to synthesize and characterize the nanocomposites by using onion extract as reducing agent. The synthesized nanocomposites were characterized by UV-VIS spectrophotometer, scanning electron microscope (SEM), Energy Dispersive X-ray spectroscopy (EDAX), Fourier transform infra-red spectroscopy (FTIR), X-ray diffraction pattern (XRD) and Zeta potential analyses. The results revealed that the onion extract was found to be a successful reducing agent for the synthesis of nanoparticles as nanocomposite. The synthesized nanoparticles were initially confirmed by visual observation by colour change. The metal ions were reduced during the exposure to aqueous extract of onion. Further, the nanocomposites were structurally and chemically characterized by various techniques.

**Key words:** green, onion, Ag/ZnO, nanocomposites, synthesis, characterization

## 1. INTRODUCTION

Nanocomposites are composites in which at least one of the phases shows dimensions in the nanometre range. Nanocomposite materials have emerged as suitable alternatives to overcome limitations of microcomposites and monolithics, while posing preparation challenges related to the control of elemental composition and stoichiometry in the nanocluster phase. They are reported to be the materials of 21<sup>st</sup> century in the view of possessing design uniqueness and property combinations that are not found in conventional composites. The general understanding of these properties is yet to be reached [1], even though the first inference on them was reported as early as Gleiter [2]. Nanocomposites are composites containing different compositions or structures, where at least one of the constituent is in the nanoscale regime. In other words, nanocomposites are materials that are created by introducing nanomaterials (often referred to as filler) into a macroscopic sample material (often referred to as the matrix) [3]. After adding nanomaterials to the matrix material, the resulting nanocomposites not only exhibit enhanced electrical and thermal conductivities but also distinctive optical and dielectric properties due to their quantum size effects and surface effects [4].

Nanocomposites can be classified based on their matrix materials into three different categories *i.e.* metal matrix nanocomposites, ceramic matrix nanocomposites and polymer matrix nanocomposites. Nanocomposite of insulating materials such as glasses, ceramics or polymers with embedded metal nanoparticles are under focus because of their special structural, mechanical, electrical, linear and nonlinear optical properties. Among the nanocomposites, metal-glass nanocomposite materials exhibit interesting novel properties which include nonlinear optical behaviour, increased mechanical strength, high refractive index, electrical resistivity *etc.* Such nanocomposites containing metal nanoparticles dispersed in glass matrices have also drawn attention because of their second order non-linear effects and have applications in developing high speed and low power optical devices for future communication systems [5]. Thus, the aim of the present work was to synthesize and characterization of Ag/ZnO nanocomposites.

## 2. MATERIAL AND METHODS

### 2.1 BIOSYNTHESIS OF NANOCOMPOSITES [6]

The onion bulbs were washed with sterile distilled water and the outer covering of the bulb was manually peeled off and the fleshy part of the onion was rewashed with sterile distilled water. A part of 10 g of the onion bulb was cut into small pieces and ground using mortar and pestle with distilled water. The extraction was filtered using muslin cloth and then Whatmann No.1 filter paper. The filtrate was used as reducing agent and stabilizer. The obtained onion extract was used for the synthesis of different nanoparticles. The nanocomposite was synthesized by mixing of 10ml of onion extract and 1mM pure metals (silver nitrate and zinc nitrate). The content was incubated at room temperature for 24 hours. After the incubation period, the content was centrifuged at 10,000 rpm for 20 minutes. The pellet was collected and air dried. To 1mg of sample, 2.5 ml of 100% ethanol and 2.5 ml of double distilled water were added. The content was mixed well and 0.002 g of PEG 200 was added. The mixture was centrifuged at 8000 rpm for 10minutes. The pellet was collected and air dried. The nanocomposites thus obtained were purified by repeated centrifugation at 10000 rpm at 25°C for 10 minutes. It was followed by re-dispersion of the pellet in deionized water to get rid of any uncoordinated biological molecules. The

process of centrifugation and re-dispersion were repeated with sterile distilled water to ensure better separation of free entities from the nanoparticles.

## 2.2 CHARACTERIZATION OF NANOCOMPOSITES

The synthesized nanocomposites were characterized by UV-Visible spectroscopy [7], Scanning Electron Microscopy [8], Fourier Transform Infrared Spectroscopy [9] and Zeta potential analysis [10]. Further, to determine the nature and size of the synthesized nanoparticles, X-ray diffraction (XRD) was performed. For that the spectra were recorded 40 kV and a current of 30 mA with CuK $\alpha$  radiation using XRD (Philips PW1050/37 model). The diffracted intensities were recorded from 20°C to 80° at 2 $\theta$  angles. The crystalline nature of synthesized nanoparticles was calculated from the width of the XRD peaks, using the Debye-Scherrer formula:  $D = K\lambda/\beta \cos\theta$ . X-ray spectrometer (EDAX) operated at an accelerating voltage at 10 KeV. The sample was then sputter coated with gold and visualized with a BRUKER to assess the particle size, shape and percentage of synthesized particles. The XRD values were inferred through JCPDS file no 89-3722. Further, the UV-Visible spectrum, FTIR, XRD values were interpreted by using ORIGIN VERSION-8 (data analysis and graphing work space).

## 3. RESULTS

### 3.1 VISUAL OBSERVATION OF COMPOSITES

The present study revealed that the onion extract was found to be a successful reducing agent for the synthesis of nanocomposites. The synthesized nanoparticles were initially confirmed by visual observation by colour change. The metal ions were reduced during the exposure to aqueous extract of onion within 24 hours of incubation period. It was observed that the colour of the reaction mixture was changed for nanocomposite to pale yellow to black colour (Fig. 1). Further, the synthesized nanoparticles were characterized by UV-Visible spectroscopy, Fourier Transform Infrared Spectroscopy (FT-IR), X-Ray diffraction, Scanning Electron Microscope (SEM), EDAX and Zeta potential analyses.

### 3.2 UV-VISIBLE SPECTROSCOPY ANALYSIS

The reduction of metal ions in the onion extract was further confirmed by UV-Vis Spectrophotometer. UV-Vis absorption spectrum of nanocomposites was shown in (Fig. 2). The absorption spectrum of nanocomposite nanoparticles was maximum at 346nm.

### 3.3 FOURIER TRANSFORM INFRARED SPECTROSCOPY (FTIR) ANALYSIS

FTIR analysis is unique for the identification of various functional groups. FTIR analysis was carried out to identify the biomolecules which were responsible for the reduction of metal ions into their respective nanoparticles in the presence of onion extract (Fig. 3). The phytochemical found in the onion extract were responsible for the formation of various nanoparticles. The FTIR spectrum of onion extract showed several absorption peaks ranged from 3421cm<sup>-1</sup> to 677 cm<sup>-1</sup>. The region of band was phenols, alkanes due to N-H stretching of proteins and O-H stretching, > C=O stretching of esters, aromatics, ring C-C stretching of phenyl, alkanes, C-O stretch in vibration combined with the ring stretch of phenyl, aliphatic amines, alcohols, carboxylic acids, ester, ether, functional groups mainly from carbohydrate, alkyl halides. FTIR analysis for the nanocomposites showed that the absorption peaks at 3423.41cm<sup>-1</sup>, 2878.56cm<sup>-1</sup>, 1741.60cm<sup>-1</sup>, 1638.42cm<sup>-1</sup>, 1624.92cm<sup>-1</sup>, 1523.66 cm<sup>-1</sup>, 1437.83cm<sup>-1</sup>, 1368.40 cm<sup>-1</sup>, 1061.74 cm<sup>-1</sup>, 1031.85cm<sup>-1</sup>, 940.23cm<sup>-1</sup>, 763.76cm<sup>-1</sup>, 669.25cm<sup>-1</sup> and 581.50cm<sup>-1</sup>. The respective peaks were assigned for the O-H stretching vibration of H<sub>2</sub>O molecules, C-H stretching vibration, C=O stretching vibration mode of the carboxylic group for the gluconic acid, (C=O-NHR) amide group, O-H stretching, asymmetric and symmetric C-O stretching vibrations, C-O deformation of C<sub>6</sub>-OH, secondary (C<sub>6</sub>-OH) primary (C<sub>2</sub>-OH) alcohol groups, C-H and O-H deformation, assigned to CH out of plane bending vibrations are substituted ethylene -CH=CH and oxygen from hydroxyl group.

### 3.4 X-RAY DIFFRACTION (XRD) ANALYSIS

The green synthesized composite nanoparticles using onion extract were further confirmed by the characteristic peaks observed in XRD analysis (Fig. 4). The results revealed that average particle size of nanocomposite was around 5nm. The peaks in the XRD pattern could be assigned to the crystalline zinc oxide phase with the hexagonal wurzite structure with the lattice parameters a=1.593 nm and c= 1.6035 nm. In the XRD pattern, the nanocomposites were indexed at as (100), (002), (101), (102), (110), (103), (112), (201) and (202).

### 3.5 SCANNING ELECTRON MICROSCOPE (SEM) ANALYSIS

The surface morphology of the nanoparticles was characterized using Scanning Electron Microscopy. The onion extracts mediated nanocomposites found as agglomerate in nature (Fig. 5).

### 3.6 EDAX ANALYSIS

EDAX analysis is very much useful for further confirmation of presence of nanoparticles and EDAX analysis showed the confirmative peaks for nanocomposites (Fig. 6). The synthesized nanocomposites nanoparticles were confirmed by typical absorption peak at 3KeV and 1KeV respectively.

### 3.7 ZETA POTENTIAL ANALYSIS

Zeta potential measures the potential stability of the nanoparticles in the colloidal suspension. From the Zeta potential analysis, onion extracts mediated nanocomposite carry a charge of  $\pm 38.3$  mV. From this finding, the nanocomposites have good stability (Fig. 7).

## 4. DISCUSSION

### 4.1 UV-VISIBLE SPECTROSCOPY ANALYSIS

During the biosynthesis of nanocomposites, the colour of the reaction medium was changed. This colour change was reflected in the absorption spectra of composite nanoparticles. UV-visible spectroscopy is an important technique to determine the formation and stability of metal nanoparticle in aqueous solution. The reaction mixture changed the colour by adding various concentrations of metal ions. This colour change raised because of the excitation of Surface Plasmon Vibrations in the silver nanoparticle [11].

The formation of Ag NPs in the nanocomposites was determined by using the UV-visible spectroscopy, which was shown on the surface plasmon resonance (SPR) bands. The results revealed that Ag NPs started to form when  $\text{AgNO}_3/\text{Cts}/\text{PEG}$  was allowed into reaction at a moderate temperature as there was no peak at 0 h and the absorbance peak could be seen at different stirring times after the reaction started. Generally, the SPR bands are influenced by the size, shape, morphology, composition and dielectric environment of the prepared nanoparticles [12], [13]. Previous studies have shown that the spherical Ag NPs contribute to the absorption bands at around 400 nm in the UV-Vis spectra [14].

Green approach for nanostructured Ag-ZnO [15] depicts the UV-vis absorbance spectra of the pure ZnO and Ag-ZnO nanostructures. The prepared ZnO nanostructures have an absorption edge around 390 nm, which corresponded to a band gap of 3.18 eV. The spectrum of the Ag-ZnO nanostructured indicates an absorption edge around 393 nm, which corresponded to a band gap of 3.15 eV. The absorbance spectrum of the Ag-ZnO nanostructures has a typical surface plasmon resonance (SPR) peak at approximately 440 nm, indicating the presence of  $\text{Ag}^{(0)}$  NPs on the ZnO surface.

### 4.2 FTIR SPECTROSCOPY

The chemical compounds found in the onion extract were responsible for the reduction as well as stabilization of synthesized nanoparticles. FTIR has become an important tool in understanding the involvement of functional groups in relation between metal particles and biomolecules which is used to search the chemical composition of the surface of the silver nanoparticles and identify the biomolecules for capping and efficient stabilization of the metal nanoparticles [16]. The nanocomposite obtained with PEG was confirmed by FTIR spectra. Intense absorptions were observed at 1730, 1630 and  $1007\text{cm}^{-1}$ . The IR band at  $1730\text{cm}^{-1}$  was characteristic of the C=O stretching mode of the carboxylic acid group for gluconic acid. The bands due to C-O stretching mode were merged in the very broad envelope centered on 1268 and  $1007\text{cm}^{-1}$  arising from C-O, C-O-C stretches and C-O-H bends vibrations of Ag NPs in PEG. Also, the aliphatic C-H stretching, in 1413 and  $1344\text{cm}^{-1}$  were due to C-H bending vibrations [17]. After the bio-reaction  $\text{AgNO}_3$  in the PEG matrix, the created peak in  $1730\text{cm}^{-1}$  certified to the binding of -C=O for carboxylic acid and the shift in the peak at  $1007\text{cm}^{-1}$  towards lower frequency compared to peak in  $1094\text{cm}^{-1}$  for PEG was attributed to the binding of C-C-O and C-C-H groups with nanoparticles [18]. The broad peaks in 503, 407 and  $291\text{cm}^{-1}$  related to Ag NPs banding with oxygen from hydroxyl groups of PEG chains. Therefore, the FTIR spectra showed the existence of van der Waals interactions between the chain of PEG and Ag NPs in the polymeric media [19].

The typical FTIR spectrum of Ag-ZnO nanocomposite revealed that presence of broad band at  $3436.30\text{ cm}^{-1}$  corresponds to the stretching vibration of the O-H mode. This may be due to the hydroxyl groups of water on ZnO surface covering the surface of Ag. Peak at  $1639.13\text{ cm}^{-1}$  is attributed to the O-H bending mode due to adsorption of water molecules in the sample either during mixing or formation of KBr pellets [20]. The presence of additional bands at 1400, 2921.74,  $2369.57\text{ cm}^{-1}$  corresponding to stretching vibration of N-O bond in nitrate groups [21], symmetrical and asymmetrical stretching vibrations of C-H in  $\text{CH}_3$  and  $\text{CH}_2$  groups of citric acid, respectively. Peaks at 1091.30, 804.35 and  $708.7\text{ cm}^{-1}$  are assigned to Zn-O-Zn, Zn-O-H and Zn-O-Zn stretching frequencies and bending frequencies, respectively. Occurrence of significant band at  $477.75\text{ cm}^{-1}$  is characteristic of the formation of Zn-O bond [22]. Peak at  $652.17\text{ cm}^{-1}$  can be attributed to the Ag-ZnO nanocomposite formation [23].

### 4.3 XRD ANALYSIS

The typical X-ray diffraction (XRD) patterns of the pure Cts, pure PEG, Cts/PEG and the prepared Ag NPs are shown in Figure 3. Pure Cts showed two peaks at  $2\theta$  of  $9.37^\circ$  and  $19.56^\circ$  while pure PEG showed strong reflections at  $2\theta$  of  $19.23^\circ$  and  $23.34^\circ$  and weak reflections at  $13.61^\circ$  and  $27.32^\circ$ . In Cts/PEG film, the  $9.37^\circ$  reflection for chitosan is diminished which may indicate that the crystallinity of chitosan is decreased. The diffraction of PEG tended to cover the reflection of chitosan with increasing reflection at  $19.13^\circ$  in Cts/PEG film. Therefore, it was observed that Cts/PEG showed strong reflections at  $2\theta$  of  $19.13^\circ$  and  $23.20^\circ$ . For Ag/Cts/PEG NCs, the XRD peaks at  $2\theta$  of  $37.91^\circ$ ,  $43.71^\circ$ ,  $64.06^\circ$  and  $76.98^\circ$  were characteristics to the (111), (200), (220), and (311) planes of the face-centered cubic (fcc) of Ag NPs, respectively [24].

The size of the synthesized nanocomposites was analyzed by SEM. The different forms of nanoparticles were found in varying in size. The sizes of the nanoparticles were further confirmed by XRD. The X-ray diffraction analysis (XRD) patterns of the ZnO:Ag nanocomposites contains ZnO phases corresponding to the wurzite structure at  $2\theta$  values of  $31.8$ ,  $34.4$ ,  $36.3$ ,  $47.6$ ,  $56.6$ ,  $62.9$ ,  $66.4$ ,  $67.9$  and  $69.1^\circ$  in accordance with the zincite stick pattern COD 9004180. No other peak for the cubic phases of ZnO or any other ZnO structures such as  $\text{ZnO}_2$  or  $\text{Zn}(\text{OH})_4$  was seen. The Ag present in the ZnO: Ag composite nanoparticles appeared as cubic phases of pure silver crystals at  $2\theta$  values of  $38.2$ ,  $44.4$ ,  $64.5^\circ$  in accordance with reference stick pattern COD 9011607. The appearance of Ag as a separate crystal indicates that Ag is not incorporated into the wurzite structure of ZnO but preserved its crystalline form. The co-growth of ZnO wurzite and Ag cubic structures took place through the adopted in situ doping procedure. The decrease in ZnO peak heights with the increase in Ag amount indicated that ZnO crystal structure deteriorated to smaller crystallites as silver started growing as a separate phase along the ZnO crystals [25].

### 4.4 SEM ANALYSIS

The ZnO:Ag nanocomposites were hexagonal in structure containing the metallic silver on surface, with a size range of 30–40 nm. The Rutherford backscattering spectrometry (RBS) analysis of ZnO:Ag nanoparticles indicated the purity of the prepared samples with the atomic percentages of Zn, O and Ag according to the expectations. Zinc and oxygen are present in correct stoichiometric amounts indicating the presence of pure ZnO and excluding any possible presence of the  $\text{ZnO}_2$  structure. The minor variation in oxygen amount is, however, due to oxygen vacancies created by the Fermi gas we used in our annealing procedure. These oxygen vacancies gradually obtained some atmospheric oxygen when samples were stored under normal atmospheric conditions [25]. The typical SEM images were taken for the zinc tartrate precursor and Ag/ZnO composite. The zinc tartrate precursor was rod-like with an average diameter about  $1\ \mu\text{m}$  and a length up to  $10\ \mu\text{m}$ . It can be seen that the precursor morphology has been well retained and the surface became rough compared with the precursor. The microstructure of the doped nanoparticle was further investigated by TEM. The Ag/ZnO microrods consisted of plenty of nanocrystals. The nanocrystals were bound to each other to form porous structure. The nanoholes with a size of several nanometers were also clearly found, which may greatly enhance the surface area of the sample [26].

### 4.5 EDAX ANALYSIS

Energy dispersive X-ray spectroscopy (EDS, EDX or EDXRF) is an analytical technique used for the elemental analysis or chemical characterization of a sample. Further, it is used to characterize the nanoparticles composition, their shape, size and crystallinity. The surfactant (PEG 400) affected the crystallinity of ZnO nanoparticles. EDAX spectrum of ZnO and PEG 400 showed the presence of only zinc and oxygen and hence indicated the purity of ZnO nanostructures [27], [28].

#### 4.6 ZETA POTENTIAL

Zeta potential used to determine the surface potential of the silver nanoparticles synthesized using *Urtica dioica* leaves extract. Zeta potential is an essential characterization of stability in aqueous silver nanoparticles. A minimum of  $\pm 30$  mV zeta potential was required for the indication of stable silver nanoparticles. For the obtained nanoparticles, zeta values were measured and found to be  $\pm 25.1$  mV with a peak area of 100% intensity. These values provided the full stabilization of the nanoparticles, which may be the main reason in producing particle sizes with a narrow size distribution index [29]. Zeta potential is an essential parameter for the characterization of stability in aqueous nano suspension. A minimum of + 30 mV zeta potential values is required for indication of stable nano suspension. Higher zeta potential indicates greater stability of the synthesized silver nano particles [30]. Zeta potential is a physical property which is given the net surface charge of the nanoparticles, when these particles inside the solution repelling each other's since produced Coulomb explosion between the charges of the nanoparticles giving rise to no tendency for the particles to agglomerate. The criteria of stability of NPs are measured when the values of zeta potential ranged from higher than +30 mV to lower than -30 mV [31]. Surface zeta potentials were measured using the laser zeta meter. The criteria of stability of NPs are measured when the values of zeta potential ranged from higher than +30 mV to lower than -30 mV [32].

#### 5. CONCLUSION

Based on the findings of present study, it is clear that the onion extract was found to be a successful reducing agent for the synthesis of nanocomposite. Surface morphology of the synthesized nanocomposites nanoparticles were identified from SEM electron micrograph and identified as agglomerate in nature. The chemical compositions of nanocomposites were obtained from EDAX spectrum. The elemental composition from the EDAX spectrum confirmed the presence of Zn, O and Ag in the sample. From the Zeta potential analysis, it was suggested that the surface of the nanoparticles were negatively charged and dispersed in the medium and the negative value confirms the repulsion among the nanocomposites and proves that they are very stable.

#### ACKNOWLEDGMENT

The authors are thankful to the Management and the Principal of Ayya Nadar Janaki Ammal College, Sivakasi, Tamil Nadu, India for providing laboratory facilities and financial assistance to carry out this research work.

#### REFERENCES

1. D. Schmidt, D. Shah, E. P. Giannelis, "New advances in polymer/layered silicate nanocomposites," *Current Opinion in Solid State & Materials Science*, 2002, vol. 6, no. 3, pp. 205-212.
2. H. Gleiter, "Materials with ultrafine microstructures: retrospectives and perspectives," *Nanostructured Materials*, 1992, vol. 1 no. 1, pp. 1-19.
3. I. M. Manocha, Valand, Jignesh, Patel, Nikesh, Warriar, Asis and Manocha, "Nanocomposites for structural application," *Indian Journal of Pure & Applied Phisycs*, 2006, vol. 44, pp.135-142.
4. P. H. C. C. Camargo, K. G. Satyanarayana, and F. Wypych, "Nanocomposites: Synthesis, Structure, Properties and New Application Opportunities," *Materials Research*, 2009, vol. 12, no. 1, pp. 1-39.
5. P. Chakraborty, "Metal nanoclusters in glasses as non-linear photonic materials." *J. Mat. Sci.*, 1998, vol. 33, no. 9, pp. 2235-2249.
6. J. Y. Kim, M. Kim, H. M. Kim, J. Joo and J. H. Choi, "Electrical and optical studies of organic light emitting devices using swcnts-polymer nanocomposites," *Opt. Mat*, 2009, vol. 21, no. 1-3, pp. 147-151.
7. S. Roy, M. Triparna, T. Shatarupa, and P. Das, "Biosynthesis, characterization and antifungal activity of silver nanoparticles synthesized by the fungus *Aspergillus foetidus* MTCC8876. Dig.," *J. Nanomater Biostruct*, 2013, vol. 8, pp. 197-205.
8. M. Forough and K. Farhadi, "Biological and green synthesis of silver nanoparticles," 2010, *Turkish J. Eng. Env, Sci*, vol. 34, pp. 281 - 287.
9. T. C. N. Prathna, A. M. Chandrasekaran, A. Raichur and Mukherjee, "Biomimetic synthesis of silver nanoparticles by Citrus limon (Lemon) aqueous extract and theoretical prediction of particle size," *Colloid. Surf. B: Bioint*, 2011, vol. 82, pp. 152-159.
10. J. Mohammed, Haider and M. S. Mehdi, "Study of morphology and Zeta Potential analyzer for the silver nanoparticles," *Int. J. Scienti. Engineer. Res*, 2014, vol. 5, no. 7, pp. 381-387.
11. P. Mulvaney, "Surface plasmon spectroscopy of nanosized metal particles," *Langmuir*, 1996, vol. 12, pp. 788-800.
12. K. L. Kelly, E. Coronado, L. L. Zhao and G. C. Schatz, "The optical properties of metal nanoparticles: The influence of size, shape and dielectric environment," *J. Phys. Chem*, 2003, vol. 107, pp. 668-677.

13. U. Kreibig, M. Vollmer, "Optical Properties of Metal Clusters, Springer, Berlin, Germany, 1995, pp. 14–41.
14. K. G. Stamplecoskie, J. C. Scaiano, "Light emitting diode can control the morphology and optical properties of silver nanoparticles," *J. Am. Chem. Soc.* 2010, vol. 132, pp. 1825–1827.
15. S. S. Patil, R. H. Patil, S. B. Kale, M. S. Tamboli, J. D. Ambekar, W. N. Gade, S. S. Kolekar and B. B. Kale, "Nanostructured microspheres of silver zinc oxide: An excellent impediment of bacterial growth and biofilm," *J. Nanoparticle Res.* 2014, vol. 16, pp. 1–11.
16. H. Padalia, P. Moteriya and S. Chanda, "Green synthesis of silver nanoparticles from marigold flower and its synergistic antimicrobial potential," *Arab. J. Chem.* 2014, vol. 1, no. 8, 17–19.
17. S. Tunc and O. Duman, "The effect of different molecular weight of poly (ethylene glycol) on the electrokinetic and rheological properties of Na-bentonite suspensions," *Colloid. Surf. A*, 2008, vol. 317, pp. 93–99.
18. D. Philip, "Honey mediated green synthesis of gold nanoparticles," *Spectrochim. Acta A Mol. Biomol. Spectrosc.* 2009, vol. 73, pp. 650–653.
19. K. Gupta, P. C. Jana and A. K. Meikap, "Optical and electrical transport properties of polyaniline-silver Nanocomposites," *Synth. Met.* 2010, vol. 160, pp. 1566–1573.
20. R.A. Nyquist, R. Kagel, "Infrared Spectra of Inorganic Compounds," Academic Press Inc., New York/London, 1971.
21. M. S. Chauhan, R. Kumar, A. Umar, S. Chauhan, G. Kumar and M. Faisal, "Utilization of ZnO nanocones for the photocatalytic degradation of acridine orange," *J. Nanosci. Nanotechnol.* 2011, vol. 11, no. 5, pp. 4061–4066.
22. W. Liao, A. Gu, G. Liang and L. Yuan, "New high performance transparent UV-curable poly(methyl methacrylate) grafted ZnO/silicone-acrylate resin composites with simultaneously improved integrated performance," *Colloids Surf. A: Physicochem. Eng. Aspects*, 2012, vol. 396, pp. 74–82.
23. A. Jafari, M. Ghane and S. Arastoo, "Synergistic antibacterial effects of nano zinc oxide combined with silver nanocrystals," *Afr. J. Microbiol. Res.* 2011, vol. 5, pp. 5465–5473.
24. S. Arooj, S. Nazir, A. Nadhman, N. Ahmad, B. Muhammad, I. Ahmad, K. Mazhar and R. Abbasi, "Novel ZnO: Ag nanocomposites induce significant oxidative stress in human fibroblast malignant melanoma (Ht144) cells," *Beilstein J. Nanotechnol.* 2015, vol. 6, pp. 570–582.
25. S. K. Li, Y. H. Shen, A. J. Xie, X. R. Yu, L. G. Qiu, L. Zhang, Q. F. Zhang, "Green synthesis of silver nanoparticles using Capsicum Anuum L. extract," *Green Chem.* 2007, vol. 9, pp. 852–858.
26. L. Zung, L. Jiang and Y. Ding, "Investigation into antibacterial behaviour of suspensions of ZnO nanoparticles against Coli," *J. Nanopart. Res.* 2010, vol. 12, pp. 1625–1636.
27. J. S. Tan, Y. Z. Long, M. M. Li, "Preparation of aligned polymer micro/nano- fibers by electrospinning," *Chin. Phys. Lett.* 2008, vol. 25, no. 8, pp. 3067–3070.
28. Y. Lu, Y. Lin, D. Wang, L. Wang, T. Xie and T. Jiang, "Surface charge transfer properties of high-performance Ag-decorated ZnO photocatalysts," *J. Phys. D: Appl. Phys.* 2011, vol. 44, pp. 315–322.
29. J. Mohammad, Hajipour, K. M. Fromm, A. A., Ashkarran, I. R. de Larramendi, T. Rojo, V. Serpooshan, W. J. Parak and M. Mahmoudi, "Antibacterial properties of nanoparticles", *Trends Biotechnol.* 2012, vol. 30, pp. 10.
30. I. E. T. Jebakumar, M. G. Sethuraman, "Instant green synthesis of silver nanoparticles using Terminalia chebula fruit extract and evaluation of their catalytic activity on reduction of methylene blue," *Process Biochemistry*, 2012, vol. 47, pp. 1351–1355.
31. Y. Zhang, M. Yang, N.G. Portney, D. Cui, G. Budak, E. Ozbay, M. Ozkan, C. S. Ozkan, "Zeta Potential: A Surface Electrical Characteristic to Probe the Interaction of Nanoparticles with Normal and Cancer Human Breast Epithelial Cells, *Biomed. Microdevices*, 2008, vol. 10, pp. 321–328.
32. E. Akman, B. Genc Oztoprak, M. Gunes, E. Kacar, A. Demir, "Effect of Femtosecond Ti:Sapphire Laser Wavelengths on Plasmonic Behaviour and Size Evolution of Silver Nanoparticles," *Photon Nanostruct. Fundam Appl.* 2011, vol. 9, pp. 276–286.



Fig-1: Visual observation of synthesis of Nanocomposite

A-Onion

B-AgNO<sub>3</sub>+Zn(NO<sub>3</sub>)<sub>2</sub>+PEG200

C-Nanocomposite

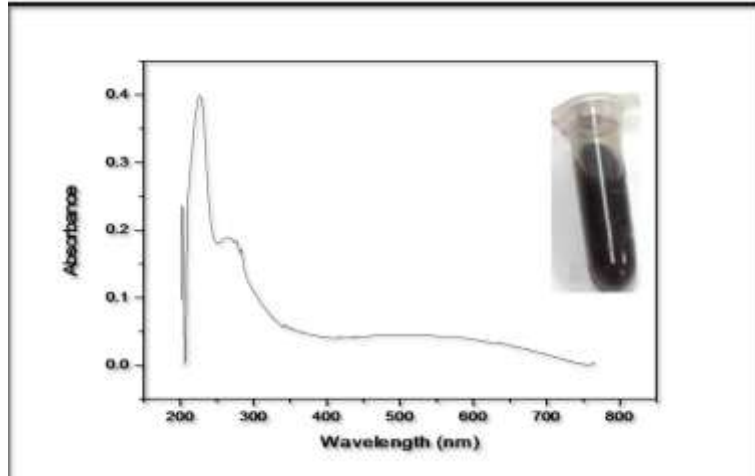


Fig-2: UV-Visible spectrum of Nanocomposites

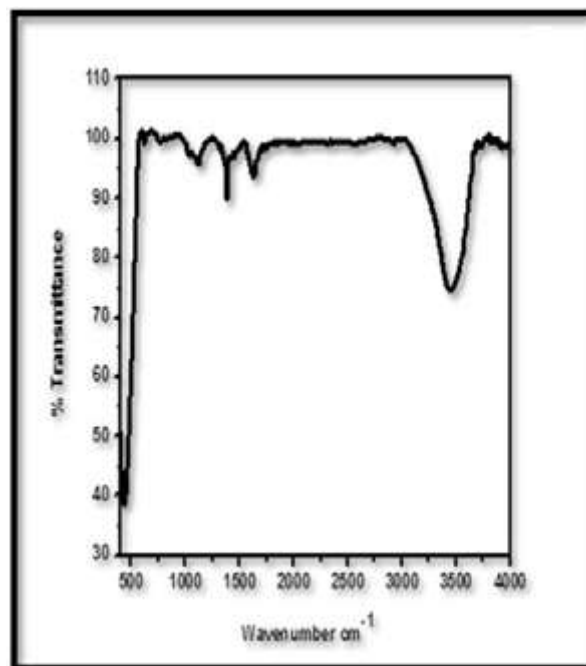


Fig-3: FTIR spectrum of Nanocomposites

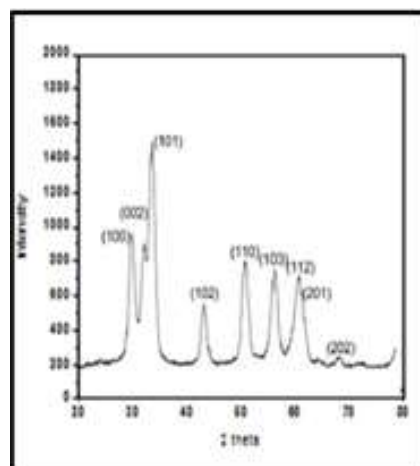


Fig-4: XRD spectra of synthesized Nanocomposites

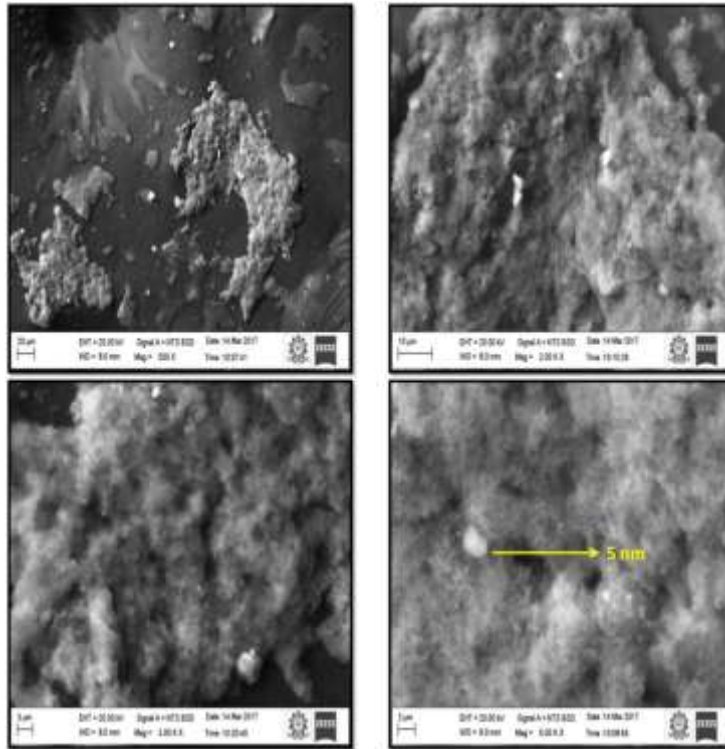


Fig-5: SEM micrograph of Nanocomposites at different magnifications

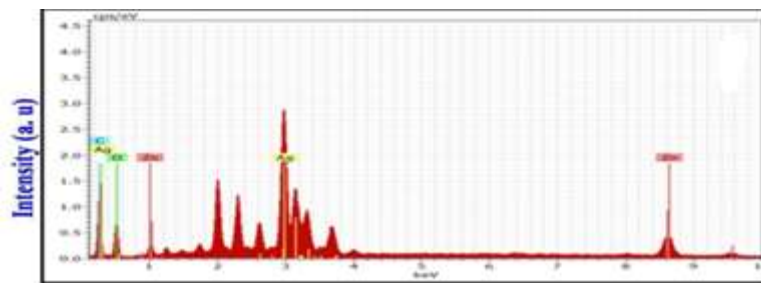


Fig-6: EDAX spectrum of Nanocomposites

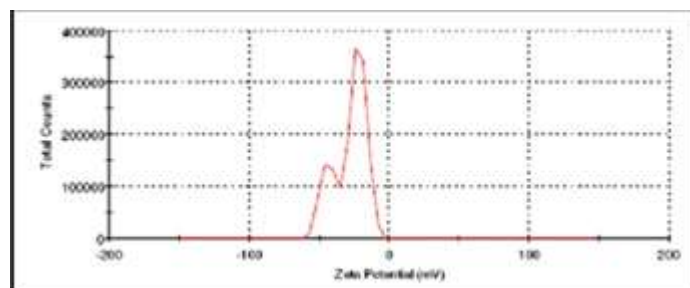


Fig-7: Zeta potential spectrum of Nanocomposites